

# Activity-based contact network scaling and epidemic propagation in metropolitan areas

Authors

<sup>1</sup> **1. Age dependent transition probabilities for the modified SEIRD model**

<sup>2</sup> For ease of reference, we briefly represent the model and the variables representing the probability of transition  
<sup>3</sup> between various states.

- <sup>4</sup> •  $S$ : susceptible
- <sup>5</sup> •  $E$ : exposed (infected, not contagious)
- <sup>6</sup> •  $I^S$ : infectious, symptomatic (clinical)
- <sup>7</sup> •  $I^A$ : infectious, asymptomatic (subclinical)
- <sup>8</sup> •  $R$ : recovered
- <sup>9</sup> •  $D$ : deceased

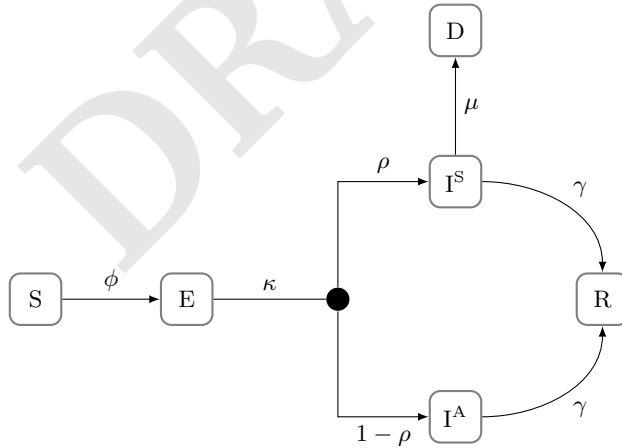


**Fig. 1.** Susceptible-Exposed-Infectious-Recovered-Deceased epidemiological model framework.  $\phi$  is the transmission probability, while  $\kappa$  is the probability of transitioning from an exposed state to an infectious one.  $\rho$  is the age-dependent probability that an infectious individual will be symptomatic.  $\mu$  is probability that an infectious individual will be deceased, while  $\gamma$  is the probability of recovery.

<sup>10</sup> The transitions to each of these states are governed by the probabilities as shown in Figure 1. In this section,  
<sup>11</sup> we limit our discussion to  $\rho$  and  $\mu$  since these two variables have been reported as highly age-dependent (1).  
<sup>12</sup> All the other transition variables (*viz.*  $\phi$ ,  $\kappa$  and  $\gamma$ ) are modeled as being independent of the age of the agent.  
<sup>13</sup> We refer to Table 1 and obtain the agent-specific value of  $\rho$  using the agent's age. Prior to starting the  
<sup>14</sup> simulation, we use this value of  $\rho$  to mark the agents for their transition to  $I^A$  or  $I^S$ . This implies, should an  
<sup>15</sup> agent become infected ( $E$ ) during the course of the simulation, his transition to  $I^A$  or  $I^S$  is predetermined.

Age	$\rho$
0-9	0.4
10-19	0.4
20-29	0.8
30-39	0.8
40-49	0.8
50-59	0.8
60-69	0.8
70-79	0.8
$\geq 80$	0.8

**Table 1.** Age related values of the probability of symptomatic infectiousness,  $\rho$ , obtained from (1) based on measurements taken in China. With more granular data, these can be updated for greater detail in simulating the epidemic across various age groups.

Given that case fatality rate (CFR) has been shown to differ significantly by age group, we use the values estimated by (2), who provide adjusted posterior mode estimates of the CFR, given measurementst over 41 days, along with 95% credible intervals. We assume the CFR is obtained from the CDF of an underlying exponential distribution governing the duration from onset of COVID-19 to death. Thus:

$$P(T > 41) = \text{CFR} \quad [1]$$

$$1 - e^{-41/d_D} = \text{CFR} \quad [2]$$

$$\implies \hat{d}_D = -\frac{t}{\ln(1 - \text{CFR})} \quad [3]$$

The value of  $d_D$  computed from the above equation is taken as the median of the lognormal random variate. Thus, the mean of the associated normal distribution is obtained by  $\mu_{\ln d_D} = \ln(\hat{d}_D)$ . We also compute the variance of  $d_D$  using the sample sizes and credible intervals computed by (2) to compute upper and lower bounds for  $d_D$ . Finally, we estimate the variance of the associated normal distribution, that is  $\sigma_{\ln d_D}^2$  by solving the transcendental equations relating the parameters of the lognormal distribution to those of the associated normal distribution. A summary of the parameters are shown in Table 2.

Age	Sample Size	CFR (95% CI)	$\hat{\mu}_{\ln d_D}$ (95% CI)	$\hat{\sigma}_{d_D}$	$\hat{\sigma}_{\ln d_D}$
0-9	$4.160 \cdot 10^2$	$2.600 \cdot 10^{-5}$ ( $3.120 \cdot 10^{-6}$ , $3.820 \cdot 10^{-4}$ )	$6.782 \cdot 10^7$ ( $1.314 \cdot 10^7$ , $1.073 \cdot 10^5$ )	$1.427 \cdot 10^1$	1.942
10-19	$5.490 \cdot 10^2$	$1.400 \cdot 10^{-4}$ ( $2.880 \cdot 10^{-5}$ , $7.590 \cdot 10^{-4}$ )	$8.186 \cdot 10^6$ ( $1.424 \cdot 10^6$ , $5.400 \cdot 10^4$ )	$1.259 \cdot 10^1$	1.830
20-29	$3.619 \cdot 10^3$	$6.000 \cdot 10^{-4}$ ( $3.170 \cdot 10^{-4}$ , $1.320 \cdot 10^{-3}$ )	$1.508 \cdot 10^6$ ( $1.293 \cdot 10^5$ , $3.104 \cdot 10^4$ )	$1.113 \cdot 10^1$	1.765
30-39	$7.600 \cdot 10^3$	$1.460 \cdot 10^{-3}$ ( $1.030 \cdot 10^{-3}$ , $2.550 \cdot 10^{-3}$ )	$5.277 \cdot 10^5$ ( $3.979 \cdot 10^4$ , $1.606 \cdot 10^4$ )	$1.024 \cdot 10^1$	1.720
40-49	$8.571 \cdot 10^3$	$2.950 \cdot 10^{-3}$ ( $2.210 \cdot 10^{-3}$ , $4.220 \cdot 10^{-3}$ )	$2.087 \cdot 10^5$ ( $1.853 \cdot 10^4$ , $9.695 \cdot 10^3$ )	9.538	1.656
50-59	$1.001 \cdot 10^4$	$1.250 \cdot 10^{-2}$ ( $1.030 \cdot 10^{-2}$ , $1.550 \cdot 10^{-2}$ )	$3.408 \cdot 10^4$ ( $3.960 \cdot 10^3$ , $2.625 \cdot 10^3$ )	8.089	1.548
60-69	$8.583 \cdot 10^3$	$3.990 \cdot 10^{-2}$ ( $3.410 \cdot 10^{-2}$ , $4.550 \cdot 10^{-2}$ )	$7.121 \cdot 10^3$ ( $1.182 \cdot 10^3$ , $8.804 \cdot 10^2$ )	6.915	1.423
70-79	$3.918 \cdot 10^3$	$8.610 \cdot 10^{-2}$ ( $7.480 \cdot 10^{-2}$ , $9.990 \cdot 10^{-2}$ )	$2.201 \cdot 10^3$ ( $5.274 \cdot 10^2$ , $3.896 \cdot 10^2$ )	6.121	1.296
$\geq 80$	$1.408 \cdot 10^3$	$1.340 \cdot 10^{-1}$ ( $1.120 \cdot 10^{-1}$ , $1.590 \cdot 10^{-1}$ )	$1.038 \cdot 10^3$ ( $3.452 \cdot 10^2$ , $2.368 \cdot 10^2$ )	5.652	1.195

**Table 2.** Age-dependent case fatality rate (CFR) parameters. The number of days from onset to death  $d_D$  is assumed to be lognormally distributed. The CFR (95% CI) and sample size for respective age categories are obtained from (2). The reported CFR values are taken as the CDF of an exponential distribution with mean rate of occurrence  $\frac{1}{d_D}$  at day 41. The computed  $d_D$  is then taken as the median of the associated lognormal distribution, from which the parameters of the associated normal distribution,  $\hat{\mu}_{\ln d_D}$  and  $\hat{\sigma}_{\ln d_D}$ , are computed.

21

## 2. Modeling contact intensity

To properly model the contact intensity, we need to estimate the mean distance between agents (persons) at each node or vehicle. For any location where interaction might occur, we model the distances between agents by assigning them random locations within the area. The vehicles and nodes are treated differently.

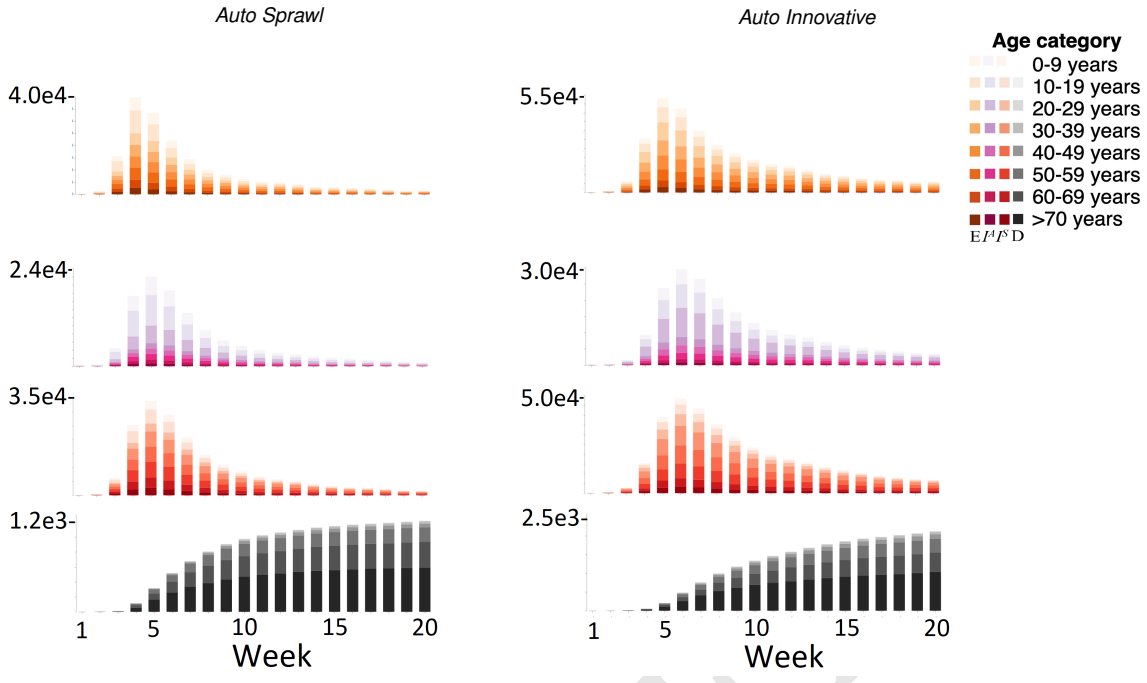


**Fig. 2. Propagation of COVID-19 by age.**

**A. Distances between agents in vehicles.** In the case of public transit vehicles, the shape of vehicle is always a rectangle. However, we assume the exposure to be limited to the immediate square a passenger is in. Hence, we assume the area of potential exposure to be a square of size equal to the width of the vehicle. Motivated by the data on average dimensions of vehicles, we make the following assumptions for the effective area of exposure within the vehicles:

$$A_{train} = \frac{1}{5} * [\text{average area of train car}] \quad [4]$$

$$A_{bus} = \frac{1}{4} * [\text{average area of a bus}] \quad [5]$$

$$A_{PV} = \text{average area of a car} \quad [6]$$

Based on the assumptions made above, the effective number of infectious people to which an agent can be exposed to is also limited to the relevant sample of total number of infectious agents on the vehicle. If total number of infectious agents on a vehicle at any given time is given by  $N_I[\text{vehicle}]$ , the effective number( $N_{EI}[\text{vehicle}]$ ) of infectious people can be summarised as follows:

$$N_{EI}[\text{train}] = \frac{1}{5} * \frac{1}{5} * N_I[\text{train}]; \text{assuming 5 cars in a train} \quad [7]$$

$$N_{EI}[\text{bus}] = \frac{1}{4} * N_I[\text{bus}] \quad [8]$$

$$N_{EI}[\text{PV}] = N_I[\text{car}] \quad [9]$$

$$[10]$$

To each agent, we assign a random location chosen uniformly within the potential area of exposure. An illustration showing the potential exposure areas for train and buses is shown in Figure 3. This is followed by computing the Euclidean distance between the agents based on these uniformly assigned locations. For faster implementation purposes, we use the mean of Euclidean distances instead. The use of mean distances is justified because the mean Euclidean distance between two agents converges to the expected distance very fast with increasing number of agents as shown in Figure 4. (See (3) for a detailed treatment of these results).

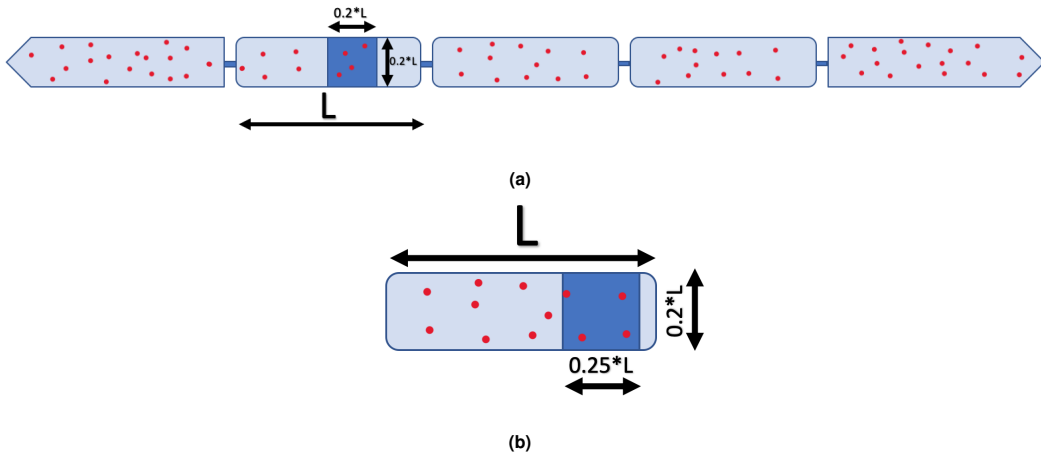


**Fig. 3.** Illustration showing assumptions for potential exposure areas in case of [Figure 3a](#): train and [Figure 3b](#): Bus

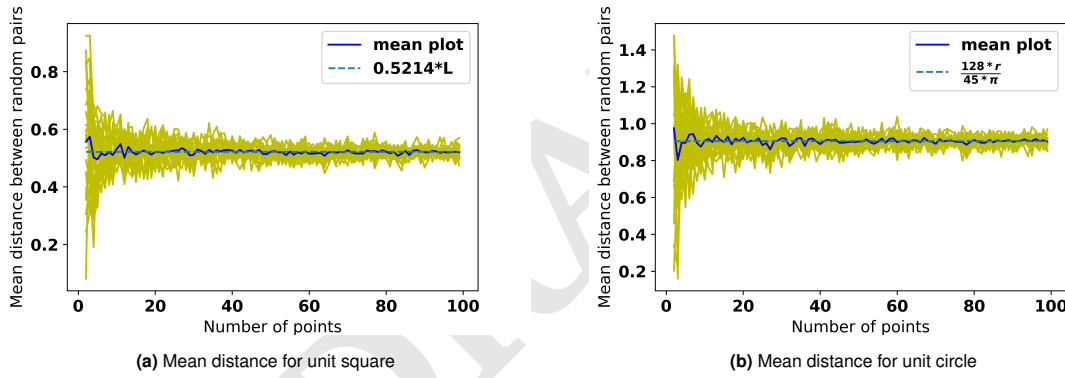


**Fig. 4.** Fast convergence of mean distance with number of points ( $N$ )

**B. Distances between agents performing activity at a node.** We partition the area of the cities into representative areas for each node of the transportation network. We use Voronoi tessellations with a clipping threshold to represent a realistic partition. The clipping threshold is selected such that post clipping, the sum of all areas, is equal to the area of the respective metros. Post clipping, a visual representation of the node-specific representative areas for both cities are shown in [Figure 7](#).

For ease of representation, we convert these node areas to circular regions of equal as shown in [Figure 6a](#). Given the number of infectious agents at the respective node ( $N_I$ ), we choose  $N_I$  points on the circle using a Gaussian centered at the centre of the circle. The variance of the Gaussian is proportional to the area of the circle. The proportion is chosen such that 95% of the points fall within the area of the circle ([Figure 6b](#)). Using this relation between variance and area, we capture the idea that the agents are distributed throughout the representative area of the node. The Gaussian nature of location assignment captures the idea that hot-spot areas of the node have a higher density of agents at any given time.

**B.1. Distances between agents staying at home.** The treatment of home is similar to a square vehicle of area  $223\text{ m}^2$ , as given by the survey from US census bureau [\(4\)](#).

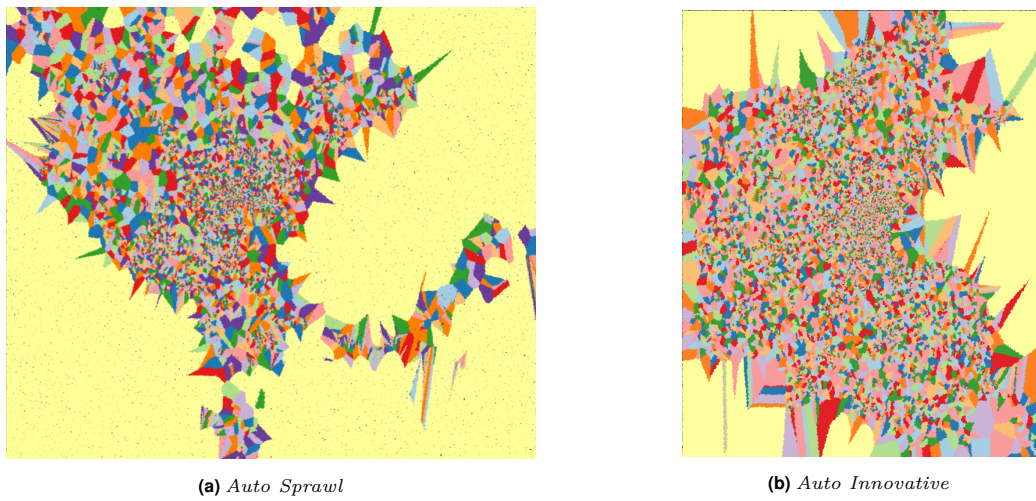
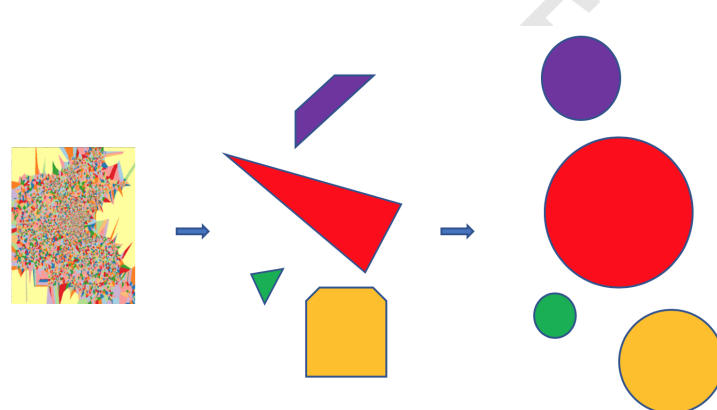
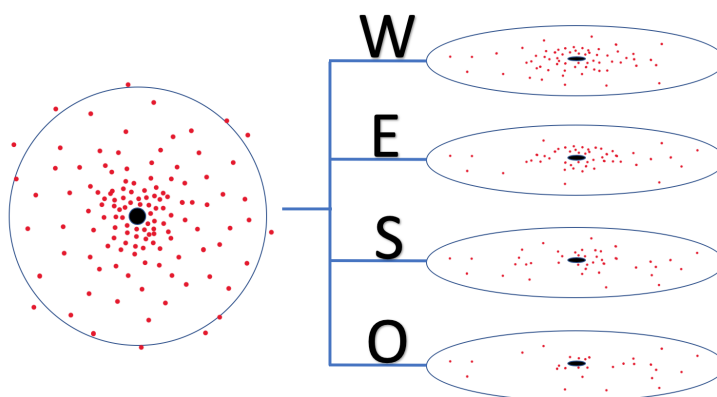


**Fig. 5.** Representative areas of nodes for each city



(a) Circular representations of Voronoi areas shown for three sample nodes



(b) Splitting of agent into layers according to activity (W: Work, E: Education, S: Shopping, O: Other)

**Fig. 6.** Assigning random locations to agents at a node

46 **3. Contact network**

47 A contact network carries information about the frequency and intensity of contacts between the agents at  
 48 different points in space and time. We accomplish the creation of the contact network from the output of  
 49 transportation simulation by separate treatment of different modes of the interaction within the network.  
 50 The interaction can be either in a stationary location (e.g. a node of the city) or while traveling. Each type  
 51 of interaction is a contact network. We create separate contact graphs for the three most relevant types of  
 52 interactions: interactions while using public transit, interactions while performing an activity at a node of the  
 53 city and interactions while staying at home. A union of these individual contact graphs gives us the full contact  
 54 network for the city. We assume that the individuals who choose to drive alone, do not come into contact with  
 55 anyone else during the course of the journey. Hence, we do not account for driving as an activity.

56 **A. Temporal split.** In order to simplify the construction of the contact network, we split the contact network  
 57 into networks at different times of the day. The temporal resolution of contact network used in our simulations  
 58 is 5 minutes. The contact network at any 5 minute window is a graph with several disconnected components,  
 59 each component being a clique as shown in [Figure 7a](#). Each clique represents a location where interaction  
 60 between agents might occur. At any given time all the agents present at a given location represent the nodes of  
 61 the clique.

62 The size of each clique is equal to the number of agents at the corresponding location. In order to handle  
 63 large number of agents, we simplify the graph structure and transform each clique to a hub-and-spoke structure  
 64 as shown in [Figure 7b](#). This transformation significantly reduces the number of edges in the graph and as  
 65 a consequence, reduces the computing resources required to carry out the simulation. The hub-and-spoke  
 66 representation is conveniently represented using the data structure discussed in [Section 6](#).

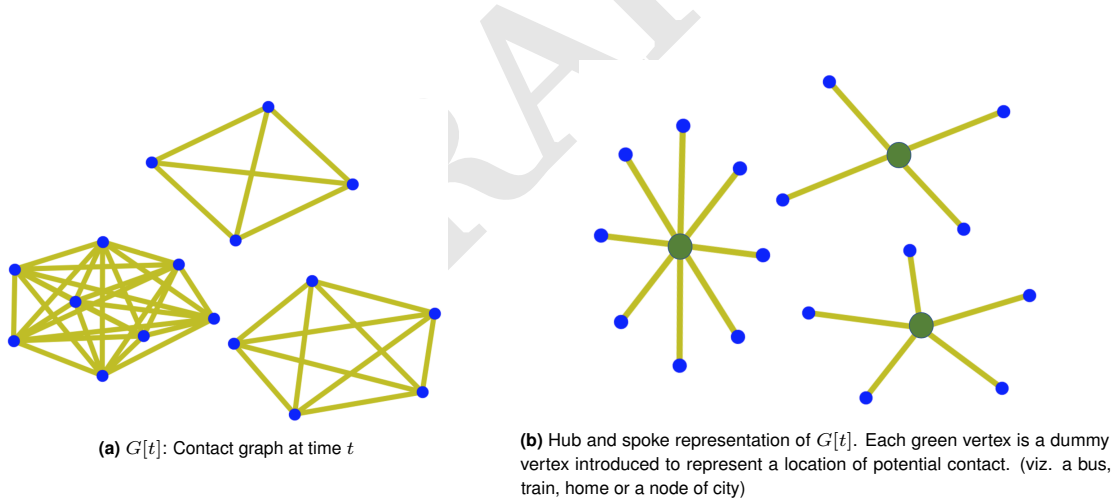


**Fig. 7.** Two representations of the contact graph. The blue vertices represent agents while green vertices represent a location. The edges are not weighted in this representation and are not linked to the intensity of contact between agents.

67 **B. Spatial split for activities.** The construction of the contact network ensures that different locations in space  
 68 are represented as a standalone component. However, the activities contact network is an exception to this.  
 69 In case of the activities network, several agents present at the same node of the city may be performing a  
 70 different class of activity, hence do not run a risk of interaction. In order to model this, we split the activity  
 71 contact network at a node into different layers based on the type of activity as shown in [Figure 6b](#). Thus, only  
 72 intra-layer interactions between agents are allowed.

73 **4. Calibration**

74 To find  $\Theta$ , we calibrate in order to achieve a basic reproductive number (average number of secondary cases  
 75 caused by an infected person in the early stage of the epidemic) of  $R_0 = 2.5$  using:

76

$$R_0 = \frac{1}{X} \sum_m^X \sum_n^S \left( 1 - e^{-\Theta'} \sum_m \tau_{nm} \right) \quad [11]$$

77 where  $\Theta' = \Theta q_0, i_0$ . We use the above equation to solve for  $\Theta'$ .

78 We notice that if we calibrate  $\Theta'$  for an  $R_0 = 2.5$  for a contact network generated using a sample of the  
 79 population, the same  $\Theta'$  does not provide a resultant  $R_0 = 2.5$  when simulating with the full population. It  
 80 results in very high values of  $R_0$ . We hypothesize that this behavior is due to the contact graph becoming  
 81 sparse when we use a small sample of the population. As building a sample of contact network happens to be  
 82 an active area of research, we leave sampling out of the scope of this work (5). We carried out our calibration  
 83 on full contact network using the entire population for both cities.

84 We also observed that the  $R_0$  is not stable when using small number of initial infections( $I_0$ ). The variation  
 85 in  $R_0$  decreases as we increase  $I_0$ . This behavior is shown in Figure 8 using three sample sizes of the population.  
 86 We observe that as the population size increases, a higher value of  $I_0$  is required to achieve a stable  $R_0$ . During  
 87 calibration, we used  $I_0 = 1000$  and while simulating the epidemic for 270 days, we started with an  $I_0 = 200$ .

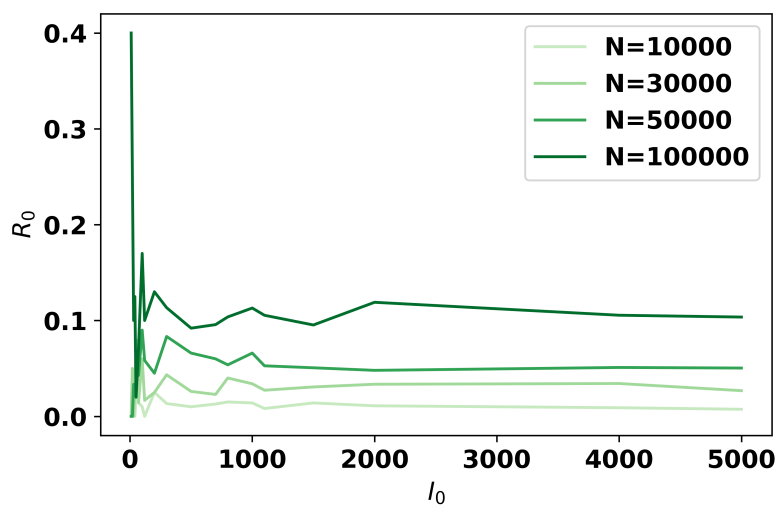


Fig. 8. Basic reproductive number  $R_0$  versus the initial number of infected agents  $I_0$  for a fixed values of  $\Theta'$ . In order to study this behavior of  $R_0$ , we sampled three different sized sets of individuals from *Auto Sprawl* and set a small  $\Theta'$ . The  $I_0$  was chosen between 0 and 5000 with more samples for smaller values.

88 **5. Performance**

89 The prototyping for this study was implemented in Python. The experiments were performed on Ubuntu  
 90 machine each core having a speed of around 1 GiB. In this section, we comment on the run times for the *Auto*  
 91 *Innovative* city. The run time of the entire script can be divided into four parts. First, the pre-processing of  
 92 the output files from the transport simulator (SimMobility in this case). This part takes around 5 minutes to  
 93 complete. Second, the creation of three sets of contact graph; Home graph, Activity graph and Transit Graph.  
 94 Each set of graphs has 288 graphs- one for each 5 minute time of the day. The creation of graphs takes around  
 95 90 minutes for a full population of 4.5 million agents in the case of *Auto Innovative*. Third, the Union operation  
 96 to combine each type of individual contact graph (*Home*, *Activity* and *Transit*) takes around 10 minutes using  
 97 10 threads in parallel. Fourth, the actual simulation for a period of 270 days takes around 9 hours.

98 There are several avenues where the performance can be improved. First, we can parallelise the graph  
99 creation process in temporal dimension. The contact graphs at different times of the day can be generated in  
100 parallel. Second, we can parallelise the actual simulation process, with each thread processing one component  
101 of the contact graph as shown in [Figure 7b](#).

102 **6. Pseudocode**

---

**Data Structure** representing a contact Graph at timestep  $t$  ( $G[t]$ )

---

At every time-step  $t$ , the contact graph  $G[t]$  is a set of two maps:  $\{forwardDicts, backwardDicts\}$

$forwardDicts$  is a Map  $\langle \text{key: } person_i, \text{value: } dummy_j \rangle$  // representing an individual ( $person_i$ ) who  
is present at a dummy location ( $dummy_j$ ) at time  $t$

---

$backwardDicts$  is a Map  $\langle \text{key: } dummy_j, \text{value: } [pid_1, pid_2, \dots, pid_{n_j}] \rangle$  // where  $n_j$  is number of  
individuals at the location  $dummy_j$  at time  $t$

---

---

### PanCitySim Framework

---

```

stateVector  $\leftarrow (S/E/I^A/I^S/R/D)$  for every person
Initialise stateVector[person] = S  $\forall$  persons
 $I_0 \leftarrow 200$ 
 $\rho_{binary} \leftarrow$  use  $\rho$  from table to mark every person for a possible transition to  $I^S$ ;

day  $\leftarrow 1$  // 270 days=9 months
while day  $\leq 270$  do
    timestep  $\leftarrow 1$  // we use 5-minute timesteps, total of 24*12=288 timesteps in a day
    while time - step  $\leq 288$  do
        G  $\leftarrow G_{UNION[timestep]}$ 
        for each dummy in G do
            for each person in G[backwardDict[dummy]] do
                if stateVector[person] =  $I^A$  then
                    countInfect  $\leftarrow$  countInfect + 1

                if dummy = activity(W/E/S/O) node then
                    area  $\leftarrow$  (voroni area of node( $A_v$ ))
                    samplelocs  $\leftarrow$  (countInfect locations in a circle using a Gaussian with  $\sigma_x = \sigma_y = 0.0572 * A_v$ )
                    referenceLoc  $\leftarrow$  (1 location in a circle using a Gaussian with  $\sigma_x = \sigma_y = 0.0572 * A_v$ )
                    meanDist  $\leftarrow$  (mean Euclidean distance between referenceLoc and samplelocs)

                if dummy = Train then
                    meanDist  $\leftarrow (A_{metro\ coach} * 0.2)^{0.5} * 0.5$ 
                    countInfect  $\leftarrow$  countInfect *  $\frac{1}{25}$ 

                if dummy = Bus then
                    meanDist  $\leftarrow (A_{Bus} * 0.25)^{0.5} * 0.5$ 
                    countInfect  $\leftarrow$  countInfect *  $\frac{1}{4}$ 

                if dummy = Home then
                    meanDist  $\leftarrow 6.5$ 

                if countInfect > 0 then
                    for each person in G[backwardDict[dummy]] do
                         $\phi_{nt} = 1 - \exp(-\Theta'_{calibrated} * \frac{1}{mean^3} * countInfect)$ 
                        if stateVector[person] = S then
                            if RAND(0, 1) <  $\phi_{nt}$  then
                                stateVector[person] = E

        for each person in stateVector do
            use  $\gamma$  for transitions  $I^S \rightarrow R$  and  $I^A \rightarrow R$ 
            use age-specific  $\mu$  for transitions  $I^S \rightarrow D$ 
            use predetermined  $\rho_{binary}$  to choose  $E \rightarrow I_A$  or  $E \rightarrow I_S$ 
            use  $\kappa$  to realise the transition according to the path chosen in previous step

```

---

- 103 1. Prem K, et al. (2020) The effect of control strategies to reduce social mixing on outcomes of the COVID-19 epidemic in Wuhan, China: A modelling study. *The Lancet Public*  
104 *Health* 0(0).
- 105 2. Verity R, et al. (2020) Estimates of the severity of coronavirus disease 2019: A model-based analysis. *The Lancet Infectious Diseases* 0(0).
- 106 3. Cohen JE, Courgeau D (2017) Modeling distances between humans using Taylor's law and geometric probability. *Mathematical Population Studies* 24(4):197–218.
- 107 4. US Census Bureau MCD (year?) Characteristics of New Housing (<https://www.census.gov/construction/chars/highlights.html>).
- 108 5. Génois M, Vestergaard CL, Cattuto C, Barrat A (2015) Compensating for population sampling in simulations of epidemic spread on temporal contact networks. *Nature*  
109 *Communications* 6(1):8860.

DRAFT

DRAFT